



## A study of the pressure vessel steel of the WWER-440 unit 1 of the Kozloduy nuclear power plant

E. Kostadinova<sup>1</sup> · N. Velinov<sup>2</sup> · T. Avdjieva<sup>1</sup> · I. Mitov<sup>2</sup> · V. Rusanov<sup>3</sup>

© Springer International Publishing AG, part of Springer Nature 2017

**Abstract** A comparison between highly neutron irradiated samples from the region of weld № 4 and low irradiated samples from weld № 1 taken from the pressure vessel of the WWER-440 Unit № 1 of the Kozloduy NPP has been performed. Measurements of the residual activity of samples from the outer surface of the reactor pressure vessel bottom corpus reveal very low activity of  $^{60}\text{Co}$ . Insofar as there the base and weld metal appear to be exposed to a very low neutron fluence, the samples from these locations can be considered as practically not affected and may serve as a reference basis for comparison with highly irradiated pressure vessel regions. The Mössbauer parameters isomer shift (IS) and quadrupole splitting (QS) were found to be absolutely irradiation insensitive. A stepwise reduction of the internal hyperfine magnetic field  $B_{\text{hf}}$ , each by about 2.6 T, was observed. This can be attributed to the replacement of one or two surrounding iron atoms as first nearest neighbors by non-iron alloying atoms. The Mössbauer experimental line widths for irradiated and non-irradiated samples are practically the same, which is a quite unexpected result. The area fraction ratio for the three main Zeeman sextet subspectra S1:S2:S3 shows very high irradiation sensitivity. For the bottom low irradiated region of the reactor vessel the values are S1:S2:S3 = 50.1:40.0:9.4. After seven years of operation between the pressure vessel annealing in 1989 and the autumn of 1996 when the samples from weld № 4 were taken the ratio changes strongly to S1:S2:S3 = 56.4:34.7:8.5. A possible

---

This article is part of the Topical Collection on *Proceedings of the International Conference on the Applications of the Mössbauer Effect (ICAME 2017), Saint-Petersburg, Russia, 3-8 September 2017*  
Edited by Valentin Semenov

---

✉ V. Rusanov  
rusanov@phys.uni-sofia.bg

<sup>1</sup> Department of Nuclear Engineering, University of Sofia, 5 James Bourchier Blvd., 1164 Sofia, Bulgaria

<sup>2</sup> Institute of Catalysis, BAS, Acad. G. Bonchev St., Bldg. 11, 1113 Sofia, Bulgaria

<sup>3</sup> Department of Atomic Physics, University of Sofia, 5 James Bourchier Blvd., 1164 Sofia, Bulgaria

explanation of this result is that neutron irradiation gives rise to a precipitation process involving predominantly alloying atoms as Ni, Mn, Cr, Mo and V which become mobile and precipitate in the form of carbides and/or P-rich phases and alloying atom aggregates. This “refinement” process lowers the partial area of subspectra S2 and S3 where alloying atoms are involved and leads to a higher area fraction of the pure iron component S1, which is the major experimental result. For a more complete Mössbauer investigation on the processes of generation of structure defects caused by the neutron fluence, a new series of measurements will be performed by using a set of so-called surveillance specimens with different irradiation histories which are available only for the WWER-1000 reactors of the Kozloduy NPP.

**Keywords** Reactor pressure vessel · Neutron irradiation · Radiation-induced degradation · Neutron induced hardening and embrittlement

## 1 Introduction

Reactor Pressure Vessels (RPV) operate under stress conditions: high temperature about 300 °C, high pressure over 10 MPa and intense neutron flux up to  $10^{11}$  n/(s·cm<sup>2</sup>). Low carbon alloyed steels are used as structural materials. A major problem is the degradation of the RPV steels caused by neutron irradiation. The induced defects, i.e. vacancy, edge dislocation, self and impurity interstitial atoms, substitution impurity atoms, their migration, clustering and precipitation, are not yet fully understood and are a subject of intense discussions and modeling [1]. Large numbers of such defects could lead to changes not only at microscopic atomic level, but can also affect the mechanical properties of the reactor vessel through the so-called neutron irradiation induced hardening and embrittlement. Routine destructive methods, such as Charpy V-notch or tensile tests, have been used to characterize the changes at macroscopic level. The presumption is that radiation induced defects occur first at atomic level, and therefore in order to study, understand, model and predict possible damages, experimental methods sensitive at an atomic level need to be employed. If the alloying atoms acquire thermal and neutron induced mobility, then clustering and precipitation of new iron containing components could occur. The combination of Mössbauer spectroscopy and positron annihilation spectroscopy with other analytical methods as TEM, SEM, APFIM, XRD are found to be essential tools for investigating the microstructure at an atomic scale. The properties of different eastern and western types of RPV steels and their degradation have already been studied by means of Mössbauer spectroscopy, for example [2–11].

The pressurized water reactor (WWER-440) of Unit № 1 of the Kozloduy Nuclear Power Plant (NPP) in Bulgaria was in operation between 1974 and 2002. In 1989 the Unit № 1 pressure vessel was subjected to an annealing treatment. The Russian organizations which performed this annealing procedure claimed that the operation lifetime of the pressure vessel had been restored by up to 90% [12]. In 1996 the mechanical properties and the residual lifetime of the pressure vessel were assessed through taking samples from the region of the highly neutron irradiated weld № 4. On 31.12.2002 the reactor was decommissioned.

In this contribution we present results from the first investigation in Bulgaria performed by Mössbauer spectroscopy, in parallel with other analytical methods, on samples from the highly neutron irradiated region of weld № 4 and, for comparison, from a very low neutron irradiated area of weld № 1, weld № 2 and non-irradiated reactor pressure vessel steel analogs.



**Fig. 1** Images of some of the reactor pressure vessel templates under investigation. K4 – boat-like template; K1.2 and K2.1 – parts from other boat-like templates; K1 – plate; K1.1.4 – central part of a boat-like template partially grooved on both sides and prepared for Charpy’s hammer test. In the flask – shavings of different sizes taken from the outside of weld № 1. Right-hand side – a schematic representation of the WWER-440 reactor pressure vessel. The red circles mark the regions of sampling from the very strongly neutron irradiated weld № 4 (inside) and the very low irradiation affected weld № 1 and № 2 (outside)

**Table 1** Chemical composition of base reactor corpus steel type 15X2MΦA

Chemical element, wt. %								
C	Si	Mn	Cr	Ni	Mo	V	S	P
0.13–0.18	0.17–0.37	0.30–0.60	2.50–3.08	≤0.40	0.50–0.70	0.25–0.35	≤0.025	≤0.025

## 2 Experimental details

The initial Mössbauer measurement of weld № 4 metals was performed in 2015. For this study a set of fourteen specimens from the base RPV metal steel type 15X2MΦA and the weld metal steel type 10XMΦT were available. Figure 1 presents images of some of the studied reactor vessel templates. For comparison, four specimens of the base reactor steel analog 30XГСА were also tested. The corresponding chemical composition data are summarized in Tables 1, 2 and 3. The sample material was extracted from the bulk objects via diamond filing. The samples were homogenized by mixing of 50 mg very fine (~5 μm grain size) metal powder with a small quantity of polyvinyl alcohol (PVA) and were pressed in Teflon pellets. The Mössbauer spectroscopy measurements were made in transmission geometry at room temperature with a standard spectrometer working in constant acceleration mode. Mössbauer sources of <sup>57</sup>Co in Rh matrix with activity about 25 mCi were used. The spectra were processed using the software packages CONFIT 2000 and VINDA.

X-ray energy dispersive analysis (EDAX) was performed and images in backscattered and secondary electrons were obtained for the non-radioactive samples only by means of a

**Table 2** Chemical composition of weld metal steel type 10XMΦT

Chemical element, wt. %									
C	Si	Mn	Cr	Ni	Mo	V	S	P	Ti
0.07–0.12	≤0.35	0.40–0.70	1.40–1.80	≤0.30	0.40–0.60	0.20–0.35	≤0.030	≤0.030	0.05–0.12

**Table 3** Chemical composition of base reactor corpus steel type analog

Chemical element, wt. %								
C	Si	Mn	Cr	Ni	Al	Cu	S	P
0.35	1.29	1.1	1.06	0.04	0.05	0.09	0.018	0.017

scanning electron microscope LYRA I XMU and a detector system Quantity 455, X-Flash 5010300 of BRUKER. The energy resolution of the detector system for the standard  $K_{\alpha}$  line of Mn is 127 eV.

Crystal structure studies of selected irradiated and non-irradiated samples were performed on an X-ray diffractometer type DRON 4 using filtered characteristic Cu  $K_{\alpha}$  radiation in the angle range  $2\theta$  from 30 to 120° with a step of 0.05°.

A large number of gamma-spectroscopy measurements were also made. The residual specific activities of all reactor vessel templates were determined by using a semiconductor high purity germanium detector ORTEC. For the 1332.5 keV  $^{60}\text{Co}$  line the detector relative efficiency was 33.1% and the energy resolution was about 1.7 keV. Continuous dosimetric monitoring and measurements of the equivalent dose rates at distances of 20, 50 and 100 cm were carried out by means of a dosimeter-spectrometer type HDS-101 GN.

### 3 Results and discussion

Figure 2 presents the first Mössbauer measurement of the strongly neutron irradiated sample K1 performed in 2015. Only three magnetically split subspectra with isomer shift and quadrupole splitting close to 0.0 mm/s and different magnetic Zeeman splitting are identified. Table 4 summarizes the values of the measured Mössbauer parameters. The same sample was examined by Vapirev and co-workers [13] by atomic emission spectroscopy for the content of phosphorus. Base reactor pressure vessel steels show Mössbauer spectra typical for low carbon alloyed steels, which could be successfully approximated with three Zeeman sextets. We accept the interpretation from the earliest publications of Vincze, Campbell and Aldred [14, 15] and the more recent review [16] according to which the hyperfine magnetic field (HMF) in pure base centered cubic (bcc) structure of  $\alpha$ -Fe at 23 °C is 33.0 T. Each atom has an identical chemical environment of 8 Fe as first nearest neighbors (1nn). The HMF is perturbed significantly by the presence of neighboring solute alloying atoms (X). The three sextets are related to iron atoms in  $\alpha$ -Fe structure ( $\text{Fe}_8\text{X}_0$ ) with the largest Zeeman magnetic splitting measured 33.1(1) T and iron atoms surrounded with one ( $\text{Fe}_7\text{X}_1$ ) and two ( $\text{Fe}_6\text{X}_2$ ) non-iron atoms as first nearest neighbors. A stepwise reduction of the HMF, each by about 2.6 T, was observed. No large differences in the relative intensity of the subspectra or in the experimental line widths were detected in comparison to

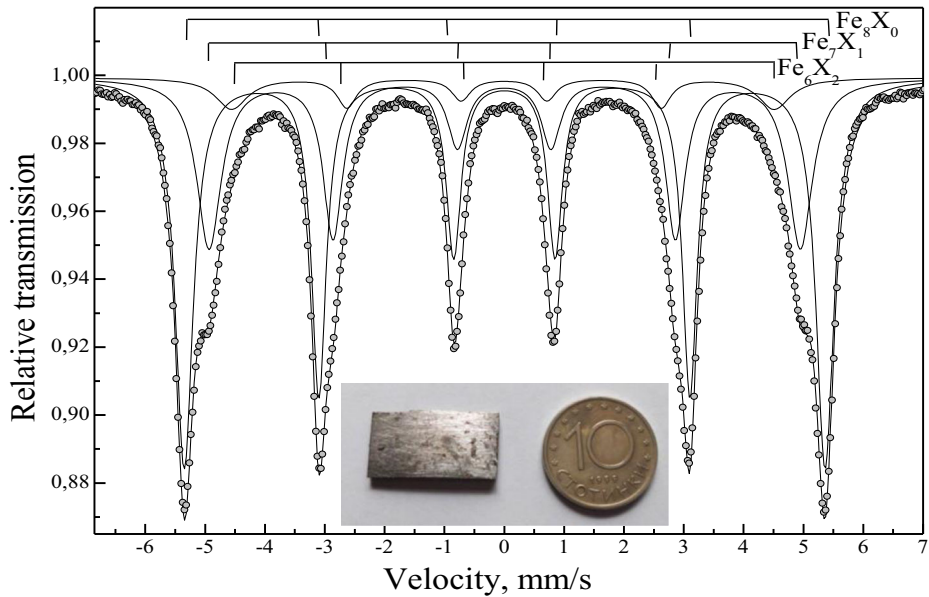


**Fig. 2** Highly neutron irradiated reactor pressure vessel steels (sample K1) show Mössbauer spectra typical for low carbon alloyed steels, which could be approximated with three Zeeman sextets

**Table 4** Values of the Mössbauer parameters: IS – isomer shift, QS – quadrupole splitting,  $B_{hf}$  – hyperfine magnetic field from the highly neutron irradiated region of weld № 4, sample K1, Fig. 2

Parameter →	IS	QS	$B_{hf}$	Area	Line width	Remarks
Subspectrum ↓	[mm/s]	[mm/s]	[T]	fraction [%]	$\Gamma_1 = \Gamma_6$ [mm/s]	
S1 ( $Fe_8X_0$ )	0.00(1)	0.00(1)	33.2(1)	57.6(1)	0.36(1)	$\alpha$ -Fe $Fe_8X_0$
S2 ( $Fe_7X_1$ )	0.00(1)	0.01(1)	30.7(1)	34.4(1)	0.49(1)	$Fe_7X_1$
S3 ( $Fe_6X_2$ )	-0.01(1)	-0.02(1)	28.2(2)	8.0(2)	0.56(2)	$Fe_6X_2$

The uncertainties of the measured values are given in brackets

non-irradiated steels of the same type (low carbon chromium steel) 25X3HM (48TC-3-40) or analogs 30XГСА. The random distribution of alloying atoms in the iron matrix was not checked by a binomial law calculation of the probability of 0, 1, 2 or 3 alloying atoms occupying nearest neighbor positions. A detailed Mössbauer study of the cation distribution in ferrites taking into account not only the first, but the influence of the second nearest neighbors and the perturbation effect of the third nearest neighbors shows a deviation in the cation distribution from the statistical and random one [17]. Moreover, in this study we will show that neutron irradiation causes changes in the subspectra area fractions and therefore in the distribution of the alloying atoms. Detailed fitting analyzes with varying the hyperfine parameter values, such as those provided in [5], were not made.

As already mentioned, a subject of major concern is the radiation-induced defects and the degradation of RPV steels caused by neutron irradiation. X-ray diffraction patterns from

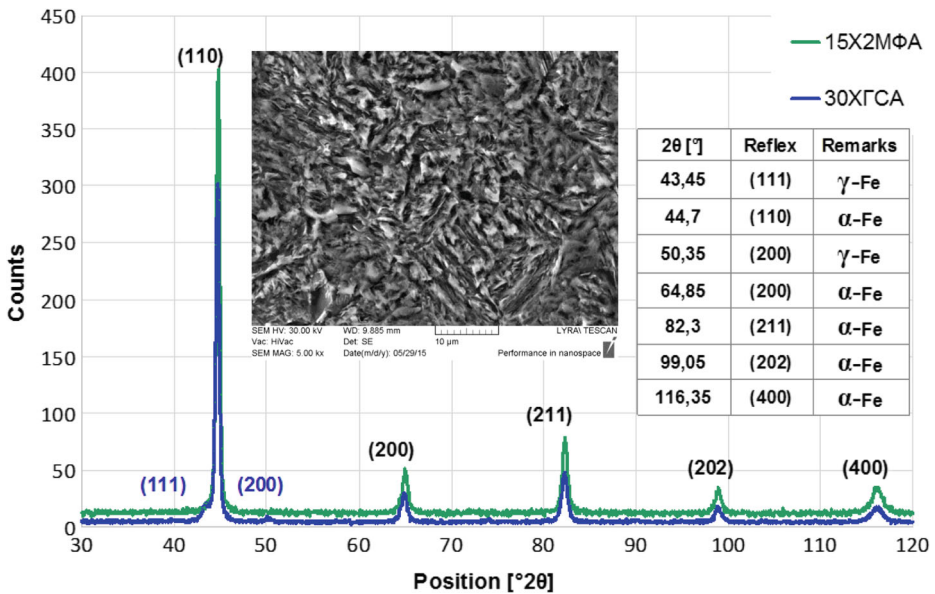


**Fig. 3** X-ray diffraction patterns from sample K1 (base reactor corpus steel type 15X2MΦA) and for comparison from reactor corpus steel analog type 30XΓCA

sample K1 (base reactor vessel steel type 15X2MΦA), and for comparison from the reactor vessel steel analog type 30XΓCA, are presented in Fig. 3, together with a scanning electron microscope image taken from a non-irradiated steel analog with typical bainite microstructure, as well as data about the main reflections and the detected phase components. The base reactor vessel steel shows only reflections from a body centered cubic bcc lattice of  $\alpha$ -Fe containing solute alloying atoms. The reactor vessel steel analog additionally shows a reflection typical for the face centered cubic fcc lattice of  $\gamma$ -Fe. The concentration of the second component (probably residual austenite) is about 10%. Reflection broadening was not observed in both samples, which is a quite unexpected result and a strong evidence for a low concentration of defects. Evidently, the seven years of operation after annealing has produced no measurable neutron irradiation induced degradation of the RPV steel. The slightly different concentrations of alloying elements cf. Tables 1 and 3, and phase compositions make the comparison between irradiated reactor vessel steel and non-irradiated vessel steel analogs uninformative.

We have found another possibility for comparison and searching for changes between irradiated and non-irradiated reactor vessel steel samples. Figure 4 presents a gamma spectrum obtained from sample K1. After twenty-one years of decay time (1996–2017) only two very intensive  $\gamma$ -lines in cascade immediately emitted from daughter isotope  $^{60}\text{Ni}$ , product of the  $\beta^-$ -decay of  $^{60}\text{Co}$  with a half time  $T_{1/2} = 5.28$  a, are detected. All other products of activation and nuclear reactions with much shorter half times in the range of days to months could not be detected today. The weak lines are artifacts: single and double escape peaks and peak of annihilation radiation. The very weak line at 1460.8 keV comes from the natural radionuclide  $^{40}\text{K}$ . The specific activity is high for all samples in the vicinity of weld № 4 – from 200 to 650 kBq/g. All samples taken from the vicinity of weld № 1 and № 2 show only a very low activity of about 5 Bq/g. The measurements of the equivalent dose rates at

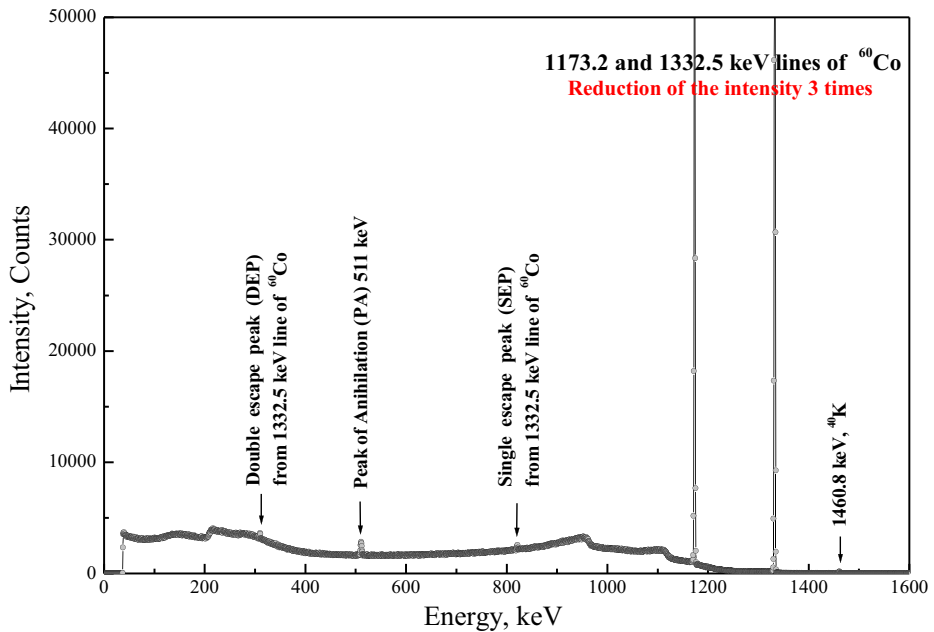
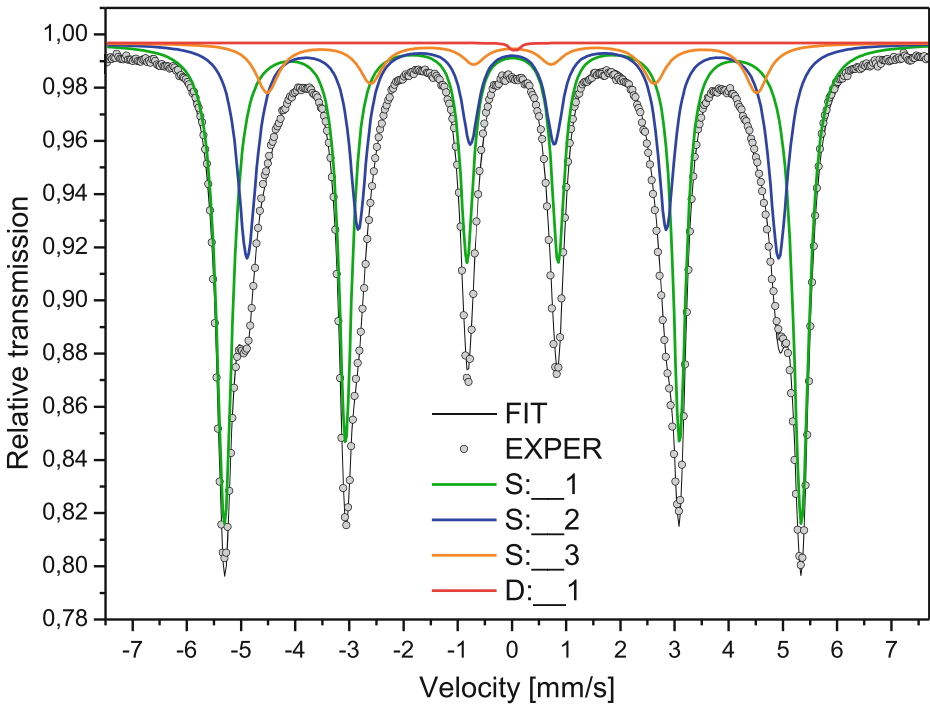


Fig. 4 Gamma spectrum received from sample K1, weld № 4

distances of 20, 50 and 100 cm from sample K1 from weld № 4 (sample weight 2.133 g) reveal maximum values of 13.95, 2.59 and 0.64  $\mu\text{Sv/h}$ . The values at all distances measured from samples weighing 21.066 g taken from the outer surface of the reactor pressure vessel bottom are 0.12  $\mu\text{Sv/h}$ , which is typically the gamma radiation background in Sofia. This result is very important and indicates that the fluence accumulated in the lower segment of the reactor vessel is roughly one hundred thousand times lower. The base and weld metal are practically not affected and could serve as reference samples for comparison with the highly irradiated region of weld № 4.

Figure 5 shows an example of a Mössbauer spectrum taken at room temperature from the highly neutron irradiated region of weld № 4. Table 5 summarizes the mean values of the Mössbauer parameters from four independent Mössbauer measurements of high statistical significance performed on samples from this region. The uncertainties of the measured values are given in brackets. An example of a Mössbauer spectrum taken at room temperature from the low neutron irradiated region of weld № 1 is presented in Fig. 6. Table 6 summarizes the mean values of the Mössbauer parameters from three independent Mössbauer measurements of high statistical significance performed on low irradiated samples. For comparison between Tables 5 and 6, the values which differ outside of the uncertainty range are given in bold. The main features are the presence of three magnetically split subspectra with isomer shift and quadrupole splitting close to 0.0 mm/s and nearly the same magnetic Zeeman splitting and experimental line widths. Only for a better approximation of the central part of the spectra, a very weak singlet line (L) or unresolved quadrupole doublet (D) were superimposed. Their area fraction is very low ( $\leq 0.5\%$ ) and we have neglected this component in the discussion and conclusions. The major experimental result is the detected change in the area fraction ratio for the three



**Fig. 5** Example for Mössbauer spectra taken at room temperature from highly neutron irradiated region of weld № 4

**Table 5** Mean values of the Mössbauer parameters: IS – isomer shift, QS – quadrupole splitting,  $B_{hf}$  – hyperfine magnetic field from four independent Mössbauer measurements of high statistical significance performed on samples from the highly neutron irradiated region of weld № 4

Parameter →	IS	QS	$B_{hf}$	Area	Line width	Remarks
Subspectrum ↓	[mm/s]	[mm/s]	[T]	fraction [%]	$\Gamma_1 = \Gamma_6$ or $\Gamma_1 = \Gamma_2$ [mm/s]	
S1 ( $Fe_8X_0$ )	0.01(1)	0.00(1)	33.1(1)	<b>56.4(1)</b>	0.34(1)	$\alpha$ -Fe $Fe_8X_0$
S2 ( $Fe_7X_1$ )	0.01(1)	0.01(1)	30.5(1)	<b>34.7(1)</b>	0.45(1)	$Fe_7X_1$
S3 ( $Fe_6X_2$ )	-0.01(1)	-0.01(1)	27.9(2)	<b>8.5(2)</b>	0.55(2)	$Fe_6X_2$
L/D	0.02/0.05(5)	0/0.2(1)	-	0.4(3)	0.4/0.3(1)	(Ni, Mn, Cr, Mo, $Fe_3C$ (P))

The uncertainties of the measured values are given in brackets. For comparison with Table 6, the values which differ out of the uncertainty range are given in bold

main Zeeman sextet subspectra S1:S2:S3, cf. Tables 5 and 6. In our opinion, this ratio exhibits a very high irradiation sensitivity and should be used in future studies as the principal parameter for quantifying of the ongoing structural changes induced by fast neutron irradiation.

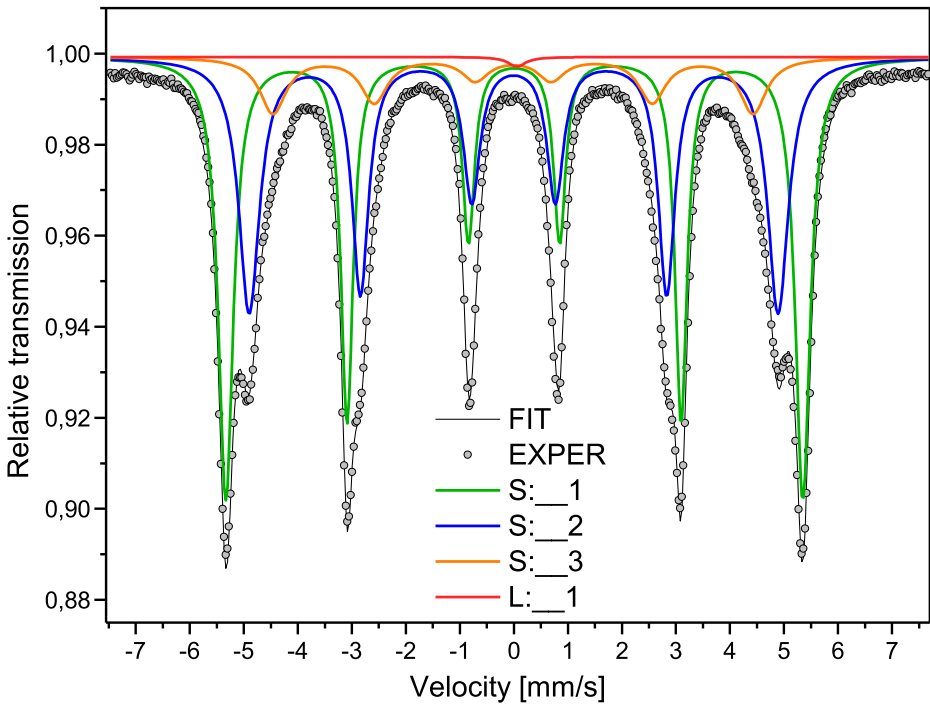


**Fig. 6** Example for Mössbauer spectra taken at room temperature from low neutron irradiated region of weld № 1

**Table 6** Mean values of the Mössbauer parameters: IS – isomer shift, QS – quadrupole splitting,  $B_{hf}$  – hyperfine magnetic field from three independent Mössbauer measurements performed at room temperature on samples from the low neutron irradiated region of weld № 1

Parameter →	IS	QS	$B_{hf}$	Area	Line width	Remarks
Subspectrum ↓	[mm/s]	[mm/s]	[T]	fraction [%]	$\Gamma_1 = \Gamma_6$ $\Gamma_1 = \Gamma_2$ [mm/s]	
S1 ( $Fe_8X_0$ )	0.00(1)	0.00(1)	33.2(1)	<b>50.1(1)</b>	0.33(1)	$\alpha$ -Fe $Fe_8X_0$
S2 ( $Fe_7X_1$ )	0.00(1)	0.00(1)	30.5(1)	<b>40.0(1)</b>	0.46(1)	$Fe_7X_1$
S3 ( $Fe_6X_2$ )	-0.01(1)	-0.00(1)	27.7(2)	<b>9.4(2)</b>	0.57(2)	$Fe_6X_2$
L/D	0.06/0.04(5)	0/0.2(1)	-	0.5(3)	0.3/0.3(1)	(Ni, Mn, Cr, Mo, $Fe_3C(P)$ )

The uncertainties of the measured values are given in brackets. For comparison with Table 5, the values which differ out of the uncertainty range are given in bold

### 4 Conclusion

The comparison between highly neutron irradiated samples from the region of weld № 4 and low irradiated samples from weld № 1 taken from Unit № 1 of Kozloduy NPP leads to the following major conclusions: 1) The comparison between strongly irradiated base reactor steel and non-irradiated reactor steel analogs has been found to be uninformative.

The reason is the slightly different chemical and phase composition of the irradiated reactor steel and this of the non-irradiated steel analog. 2) Measurements of the residual activity of samples taken from the bottom of the reactor vessel reveal a very low activity of  $^{60}\text{Co}$ . This indicates that there the accumulated neutron fluence is approximately one hundred thousand times lower. The samples from this region can be considered to be practically unaffected and therefore suitable as reference ones for comparison with highly irradiated reactor vessel regions. 3) The Mössbauer parameters isomer shift IS and quadrupole splitting QS are absolutely radiation insensitive. A stepwise reduction of the internal hyperfine magnetic field  $B_{\text{hf}}$ , each by about 2.6 T, was observed. This can be attributed to replacement of one or two surrounding iron atoms as first nearest neighbors by non-iron alloying atoms. 4) The Mössbauer experimental line widths for irradiated and non-irradiated samples are practically the same, which is a quite unexpected result. This conclusion is also confirmed by the lack of reflex broadening in the X-ray diffraction patterns. 5) The area fraction ratio for the three main Zeeman sextet subspectra S1:S2:S3 shows very high irradiation sensitivity. For the low irradiated bottom region of the reactor pressure vessel the values are S1:S2:S3 = 50.1:40.0:9.4. After seven years of operation between the vessel annealing in 1989 and the autumn of 1996 when the samples from weld № 4 were taken, the ratio changes strongly to S1:S2:S3 = 56.4:34.7:8.5. One possible explanation is given in [11]. The neutron irradiation has caused a precipitation process involving predominantly alloying atoms such as Ni, Mn, Cr, Mo and V, which become mobile and precipitate in the form of carbides and/or P-rich phases and alloying atom aggregates. This “refinement” process lowers the partial area of subspectra S2 and S3 where alloying atoms are involved and leads to higher area fraction of the pure iron component S1, which is the major experimental result. 6) All known Mössbauer studies, including ours, have one significant common flaw or rather incompleteness. Single sample(s), irradiated and non-irradiated, are usually studied. There are no comprehensive Mössbauer investigations on the correspondence between the accumulation of structural defects and the progress of neutron irradiation during reactor operation. Such studies will be performed by using a set of so-called surveillance specimens with a well quantified range of irradiation histories which are available only for the WWER-1000 reactors of the Kozloduy NPP.

**Acknowledgements** We would like to thank Dr. Ivaylo Christoskov for the neutron fluence calculations, the helpful discussions and his standing interest in this work. Special thanks are due to Mr. Momchil Kazakov for his help in the recent sampling at the Kozloduy NPP. The partial financial support of the Research Fund of the University of Sofia (Contract No. 80-10-125/2017) is highly appreciated.

## References

1. IAEA-TECDOC-1545: Characterization Testing of Materials for Nuclear Reactors Proceedings of a Technical Meeting, IAEA, Vienna (2007)
2. Brauer, G., Popp, K.: Neutron embrittlement of reactor pressure vessel steels: a challenge to positron annihilation and other methods. *Phys. Status Solidi (a)* **102**, 79–90 (1987)
3. de Bakker, P.M.A., De Grave, E., van Walle, E., Fabry, A.: RPV Steel embrittlement studied by Mössbauer spectroscopy. In: Ortalli, I. (ed.) Proceedings of the International Conference on the Applications of the Mössbauer Effect ICAME'95, Rimini, 1995, vol 50, Italian Physical Society, Bologna, pp. 145–149 (1996)
4. Lipka, J., Haščík, J., Slugeň, V., Kupča, L., Miglierini, M., Gröne, R., Tóth, I., Vilásek, K., Sitek, J.: Surveillance specimen program for the reactor pressure vessel study. In: Ortalli, I. (ed.) Proceedings of the International Conference on the Applications of the Mössbauer Effect ICAME'95, Rimini, 1995, vol 50, Italian Physical Society, Bologna, pp. 161–164 (1996)

5. de Bakker, P.M.A., Slugeň, V., De Grave, E., van Walle, E., Fabry, A.: Differences between eastern and western-type nuclear reactor pressure vessel steels as probed by Mössbauer spectroscopy. *Hyperfine Interact.* **110**, 11–16 (1997)
6. Slugeň, V., Magula, V.: The micro structural study of 15kh2MFA and 15kh2NMFA reactor pressure vessel steels using positron-annihilation spectroscopy, Mössbauer spectroscopy and transmission electron microscopy. *Nucl. Eng. Des.* **186**, 323–342 (1998)
7. Slugeň, V., Segers, D., de Bakker, P.M.A., De Grave, E., Magula, V., Van Hoecke, T., Van Waeyenberge, B.: Annealing behaviour of reactor pressure-vessel steels studied by positron-annihilation spectroscopy, Mössbauer spectroscopy and transmission electron microscopy. *J. Nucl. Mater.* **274**, 273–286 (1999)
8. Kupča, L., Beňo, P.: Irradiation embrittlement monitoring of WWER-440/213 TYPE RPVs. *Nucl. Eng. Des.* **196**, 81–91 (2000)
9. Iloa, R., Nadutov, V., Valo, M., Hänninen, H.: On irradiation embrittlement and recovery annealing mechanisms of Cr–Mo–V type pressure vessel steels. *J. Nucl. Mater.* **302**, 185–192 (2002)
10. Slugeň, V., Lipka, J., Tóth, I., Hascik, J.: Mössbauer spectroscopy used for testing of reactor steels. *NDT & E International* **35**, 511–518 (2002)
11. Zeman, A., Debarberis, L., Kupča, L., Acosta, B., Kytka, M., Degmová, J.: Study of radiation-induced degradation of RPV steels and model alloys by positron annihilation and Mössbauer spectroscopy. *J. Nucl. Mater.* **360**, 272–281 (2007)
12. Berkovich, V.Ia., Nikitenko, M.P., Chetverikov, A.E., Tishin, A.N.: Vosstanovitelnoj otjig korpusov reaktora WWER-440. UDK 621.039.526.2 1–12. (in Russian)
13. Vapirev, E.I., Teneva, M., Tsokov, P., Dimitrov, L., Dimova, G., Andreev, T., Minev, L., Boshkova, T., Angelov, V.: In-depth element analysis of weld no. 4 of RPV of unit no. 1 of KzNPP (atomic emission spectroscopy). *Nucl. Eng. Des.* **191**, 341–347 (1999)
14. Vincze, I., Campbell, I.A.: Mössbauer measurements in iron based alloys with transition metals. *J. Phys. F Metal Phys.* **3**, 647–663 (1973)
15. Vincze, I., Aldred, A.T.: Mössbauer measurements in iron-base alloys with nontransition elements. *Phys. Rev. B* **9**, 3845–3853 (1974)
16. Fultz, B.: Mössbauer spectrometry. In: Kaufmann, E. (ed.) *Characterization of Materials*. Wiley, New York (2011)
17. Rusanov, V., Gushterov, V., Nikolov, S., Trautwein, A.X.: Detailed Mössbauer study of the cation distribution in  $\text{CoFe}_2\text{O}_4$  ferrites. *Hyperfine Interact.* **191**, 67–74 (2009)